Radiotherapy and Oncology 162 (2021) 162–169

Contents lists available at ScienceDirect

Radiotherapy and Oncology

journal homepage: www.thegreenjournal.com

Original Article

Seminal vesicle intrafraction motion during the delivery of radiotherapy sessions on a 1.5 T MR-Linac

D.M. Muinck Keizer de [a,*], T. Willigenburg [a], J.R.N. der Voort van Zyp van [a], B.W. Raaymakers [a], J.J.W. Lagendijk [a], J.C.J. Boer de [a]

[a] University Medical Center Utrecht, Department of Radiotherapy, Utrecht, The Netherlands

ARTICLE INFO

Article history:
Received 21 December 2020
Received in revised form 10 July 2021
Accepted 12 July 2021
Available online 20 July 2021

Keywords:
Prostate cancer
Intrafraction motion
Cine-MR
MR-guided radiotherapy
MR-Linac
Seminal vesicles

Purpose: To evaluate seminal vesicle (SV) intrafraction motion using cinematic magnetic resonance imaging (cine-MR) during the delivery of online adaptive MR-Linac radiotherapy fractions, in preparation of MR-guided extremely hypofractionated radiotherapy for intermediate to high-risk prostate cancer patients.

Material and Methods: Fifty prostate cancer patients were treated with 5 × 7.25 Gy on a 1.5 Tesla MR-Linac. 3D Cine-MR imaging was started simultaneously and acquired over the full beam-on period. Intrafraction motion in this cine-MR was determined for each SV separately with a previously validated soft-tissue contrast-based tracking algorithm. Motion statistics and coverage probability for the SVs and prostate were determined based on the obtained results.

Results: SV motion was automatically determined during the beam-on period (approx. 10 min) for 247 fractions. SV intrafraction motion shows larger spread than prostate intrafraction motion and increases over time. This difference is especially evident in the anterior and cranial translation directions. Significant difference in rotation about the left–right axis was found, with larger rotation for the SVs than the prostate. Intra-fraction coverage probability of 99% can be achieved when using 5 mm isometric expansion for the left and right SV and 3 mm for the prostate.

Conclusion: This is the first study to investigate SV intrafraction motion during MR-guided RT sessions on an MR-Linac. We have shown that high quality 3D cine-MR imaging and SV tracking during RT is feasible with beam-on. The tracking method as described may be used as input for a fast replanning algorithm, which allows for intrafraction plan adaptation.

Introduction

In recent days, a growing number of patients with prostate cancer are being treated using online magnetic resonance (MR)-guided radiotherapy. While the first patients were treated with 20 fractions [1,2], MR-guided hypofractionated prostate radiotherapy for low and intermediate risk patients with five fractions has now successfully been performed [3,4].

Previous studies on an MR-linac have shown the significance of prostate intrafraction motion [5] and its impact on the delivered dose distribution [6,7]. While intrafraction motion studies of the prostate based on cine-MR imaging [8,7] have been described extensively, literature on seminal vesicle intrafraction motion is sparse. Especially when moving to hypofractionated treatments for patients with intermediate to high-risk prostate cancer, there is a chance of possible tumor extension into the seminal vesicles [9]. To ensure adequate coverage of the seminal vesicles, margins must be based on the observed intrafraction motion.

Different studies assessed seminal vesicle intrafraction motion based on cone beam computed tomography (CBCT), such as described by Sheng et al. [10]. However, these studies were mostly limited to using start- and end-scans, which provides no real-time motion. Gill et al. [11] assessed seminal vesicle intrafraction translational motion for 11 patients based on 2D sagittal cine-MR imaging for 15 min, followed by 12 min coronal cine-MR imaging. However, to accurately determine intrafraction motion of the seminal vesicles, continuous imaging in multiple dimensions is required.

In this study, we investigate seminal vesicle and prostate intrafraction motion based on 3D cine-MR, acquired during the beam-on period of MR-guided prostate radiotherapy on a 1.5T MR-linac. To our knowledge, we are the first to report on six dimensions of freedom seminal vesicle intrafraction motion, acquired from 3D cine-MR under treatment conditions. This

* Corresponding author at: University Medical Center Utrecht, Department of Radiotherapy, Utrecht 3508 GA, The Netherlands.
E-mail address: D.M.deMuinckKeizer@umcutrecht.nl (D.M. Muinck Keizer de).

https://doi.org/10.1016/j.radonc.2021.07.014
0167-8140/

method may provide an opportunity to implement intrafraction plan adaption for patients treated with MR-guided radiotherapy, by providing the complete intrafraction motion of the target(s) to a fast replanning algorithm. In addition, we estimate seminal vesicles margins for our current workflow, based on the obtained results.

Material and methods

Fifty (50) low and intermediate risk prostate cancer patients were registered as part of an institutional review board approved registration and imaging study. Patients were treated on a 1.5 T MR-linac (Elekta Unity [12]) and underwent hypofractionated prostate radiotherapy with five fractions of 7.25 Gy over a time span of 2.5 weeks between July 2019 and May 2020 at the University Medical Center Utrecht.

Dataset and acquisition

Each MR-guided radiotherapy fraction started with the acquisition of a T2-weighted MR-scan of 2 min. This so-called pre-treatment scan was used to assess the patient's daily anatomy, i.e. interfraction changes. Delineations from the planning MR-scan or from a previous fraction were then adapted to the current scan with the use of deformable registration and adjusted were necessary to match the current anatomy. Next, plan re-optimization was started. Just prior to the end of the plan re-optimization period, a position verification (PV) T2-weighted MR-scan was obtained. This scan was used to assess whether the clinical target volume (CTV) was still within the planning target volume (PTV). When this was the case, irradiation was started.

During the beam-on period, continuous 3D cine-MR imaging was acquired with a balanced turbo field echo (bTFE) sequence. A single 3D cine-MR frame is referred to as a 'dynamic', and these so-called cine-MR dynamics have a temporal resolution of 9.4 s, a field of view of 448 × 448 × 45 voxels and an acquired voxel spacing of 2 × 2 × 2.2 mm. Exemplary slices from the cine-MR sequence are provided in Fig. 1. Additional technical details of the cine-MR sequence are provided in Table S1 of the supplementary material. Average patient treatment time (beam-on period) was 10.1 min, while the full on-couch period of a patient during a single fraction was on average 40 min. An extensive workflow description including timings was described previously [5].

Registration

Registration was based on masks created from seminal vesicle delineations. These delineations were created by a clinician for each seminal vesicle separately on the first cine-MR dynamic of every imaging dataset. All masks were thus based on delineations of the daily anatomy. An example of these delineations is provided in Figure S1, in the supplementary material.

Seminal vesicle intrafraction motion was determined by applying a mask based, rigid registration method. This method was developed from our previously published method of soft-tissue contrast-based prostate tracking [13] which was applied and validated on MR-Linac data [5]. Additional improvements were made to the original prostate registration algorithm as described in the supplementary material. These improvements allowed the method to more accurately track small volumes with relative large displacements, such as the seminal vesicles. Tracking was performed retrospectively and applied to the left and right seminal vesicle separately. The registrations were performed rigidly, and all transformations are described by a translation and rotation about the center of mass of the mask created by the clinician.

Motion in the right, posterior and cranial translation direction are given as positive values. Motion in the left, anterior and caudal direction are given as negative values. Rotation about the left–right

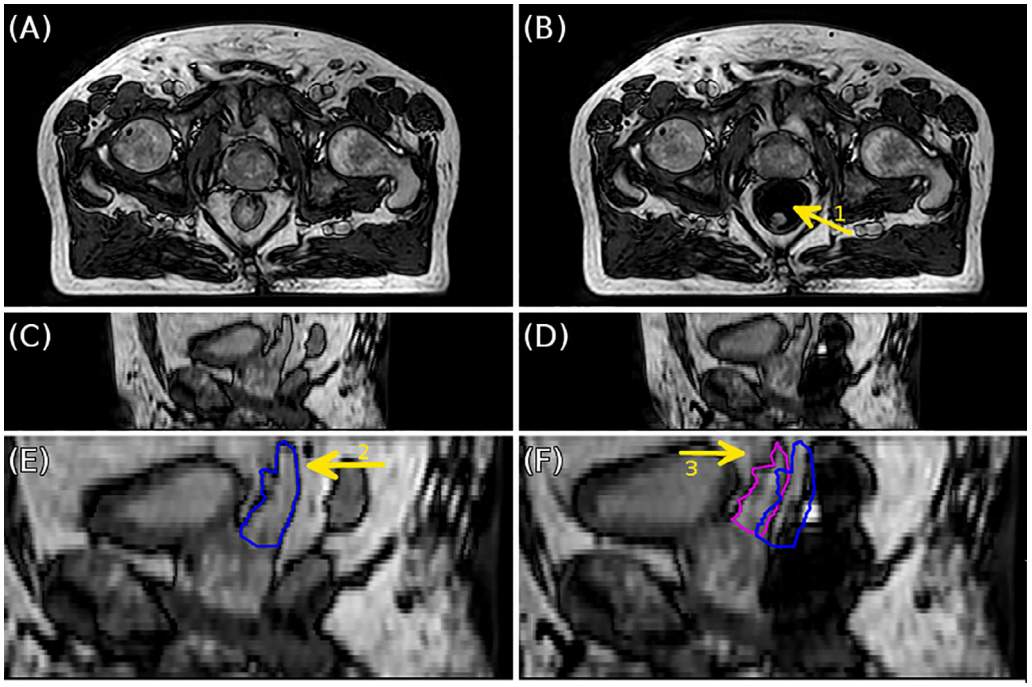

Fig. 1. Overview of cine-MR images from a single imaging session of one patient. Images A and C provide the transversal and sagittal slices at timepoint zero. Images B and D show the slices at the timepoint of 10 min. In these images, the influence of a gas pocket on the surrounding anatomy can be observed (arrow 1). Image E and F provide a sagittal close-up of the left seminal vesicle, with a delineation of the seminal vesicle in blue (arrow 2), and the found location by the tracking algorithm (cyan, arrow 3) in comparison with the original location (blue) in image F. The example provided in this figure showcases one of the largest seminal vesicle intrafraction translations seen in the dataset, with 9 mm anterior translation.

axis is equal to pitch, whereas rotation about the anterior-posterior axis is equal to roll and rotation about the caudal-cranial axis is equal to yaw rotation.

Pearson's correlation coefficients were calculated, between the intrafraction motion of both seminal vesicles and for the intrafraction motion of the seminal vesicles with respect to the prostate. Two-sample Kolmogorov–Smirnov tests were used to determine whether or not the results for the left and right seminal vesicle belonged to similar distributions. All statistical analysis was performed using MATLAB ver. R2019a.

In our previous work we reported the use of a Kalman filter in the registration pipeline [13]. This Kalman filter was also implemented in this pipeline and allows flag-raising events in case sudden changes such as large intrafraction motion or possible mis-registrations occurred. All flagged events were visually inspected to determine if a mis-registration had occurred.

Verification

The obtained intrafraction motion results were verified by applying these results as a transformation to the original mask (as created from the daily anatomy). The transformed mask was then placed on the corresponding cine-MR dynamic. If the transformed mask was visually off from the position of the seminal vesicle in the cine-MR dynamic, the result was labeled as wrong. All datasets and results were manually and systematically verified. An example of a correctly transformed mask is visualized in Fig. 1, image F.

Labeling behavior types

All cine-MR imaging sets were visually inspected and labeled to identify the major behavior type of the seminal vesicle intrafraction motion. Datasets in which gas pockets were present that influenced the seminal vesicles were labeled as "gas pockets". Datasets in which a drift occurred, due to gradual bladder filling and/or relaxation of the patient were labeled as "drift". For cases were peristalsis of the rectum or shifting rectum filling caused intrafraction motion, the label "peristalsis" was used. Remaining datasets with no visually identifiable motion behavior type and overall small amounts of seminal vesicle motion (less than 2 mm translation) were labeled as "stable". Exemplary motion paths from these groups are provided in the results.

Coverage probability analysis

The effect of intrafraction motion of the seminal vesicles and prostate during a fraction was determined using a coverage probability analysis. Such analysis describes the frequency of each target voxel being covered by a certain volume and this principle was previously described in literature [14,15]. This concept is useful because it allows taking into account rotations and deformations, whereas conventional margin recipes focus on translations only. Analysis was performed using isometric volume expansion in steps of 1 mm (range 1–10 mm), surrounding the original delineations created by the clinician.

As described previously, the obtained intrafraction motion for each cine-MR dynamic was applied with a transformation to the original mask. This results in the position of the targets corresponding with each cine-MR dynamic. A check was then performed to verify if any part of the transformed masks reached outside the expanded volume at any time point. All voxels reaching outside the expanded volume were labeled, allowing to calculate the coverage probability for each point in the original masks.

An example of this principle is provided in Fig. 4. The coverage probability analysis was performed for each target individually in all cine-MR frames and all fractions. The resulting numbers describe the percentage of volume of each target that was covered at least 95% of the time.

Population systematic (Σ) and population random (σ) graphs for the seminal vesicles and prostate center of gravity were calculated and are provided in the supplementary material. The method to determine these errors was described in a previous study [16]. The population systematic error describes the spread of the mean displacements over the group of patients at any time point. The population random error expresses the corresponding fluctuation with respect to these patient-specific means [17]. Moreover, based on these population systematic and random errors for the translation directions, calculations with the van Herk formula ($2.5\Sigma + 0.7\sigma$) [18] were performed and are provided in the supplementary material.

Results

In total, 3 complete fractions (1.2%) were excluded. This was due to failed acquisition of the cine-MR imaging due to human error (2 fractions). In one fraction the patient moved substantially during treatment, leading to significant image blurring. As an effect, the tracking algorithm was unable to analyze this specific dataset. The adopted Kalman filter flagged 139 cine-MR dynamics over 33 fractions of 18 patients. The results of 16 out of 15954 cine-MR dynamics (0.1%) involving 6 fractions of 5 patients were removed due to detected mis-registrations. In all these specific dynamics the results were visually verified and found to be incorrect.

The following results cover the remaining 247 fractions containing a total of 15938 cine-MR dynamics. The mean cine-MR acquisition duration was 10.1 ± 1.1 min (one std.). The results indicate that the prostate shows larger translational spread in the posterior and caudal translation direction (Fig. 2). However, the seminal vesicles show larger rotation about all axes than the prostate, especially about the left–right (pitch) rotation axis (Fig. 2). A distribution of the included number of samples in this analysis (cine-MR dynamics) over time is provided in Figure S2 in the supplementary material.

Pearson's correlation coefficients between the seminal vesicles with respect to the prostate in the left–right, anterior-posterior and caudal-cranial translation direction were 0.63, 0.74 and 0.72, respectively. The complete set of the Pearson's correlation coefficients with the 95 percentile confidence interval are provided in Table S2 and S3 of the supplementary material. Pearson scatter graphs for all translation and rotation directions are provided in Figure S3 and S4 of the supplementary material. In addition, histograms showing the distribution of intrafraction motion results of each target in the translation and rotation directions are provided in Figure S5 and S6 of the supplementary material.

Results of the two-sample Kolmogorov–Smirnov test indicate that for almost all timepoints the intrafraction motion of the seminal vesicles come from populations with the same distribution at 5% significance level. However, this is not the case for the timepoints after 5 min for the anterior-posterior (roll) rotation direction and the caudal-cranial (yaw) rotation direction. Full details are provided in Table S4 of the supplementary material.

The most commonly observed major motion component was peristalsis, observed in 40% of all fractions and in 84% of all patients. Drift was observed in 30% of all fractions and in 76% of all patients. Interestingly, gas pockets were found to be the major motion component in 18% of the fractions, but were observed in 50% of the patients. Only 12% of the fractions were labeled to have a stable anatomy, with less than 2 mm intrafraction motion (Table 1). Exemplary paths of these motion types are provided in

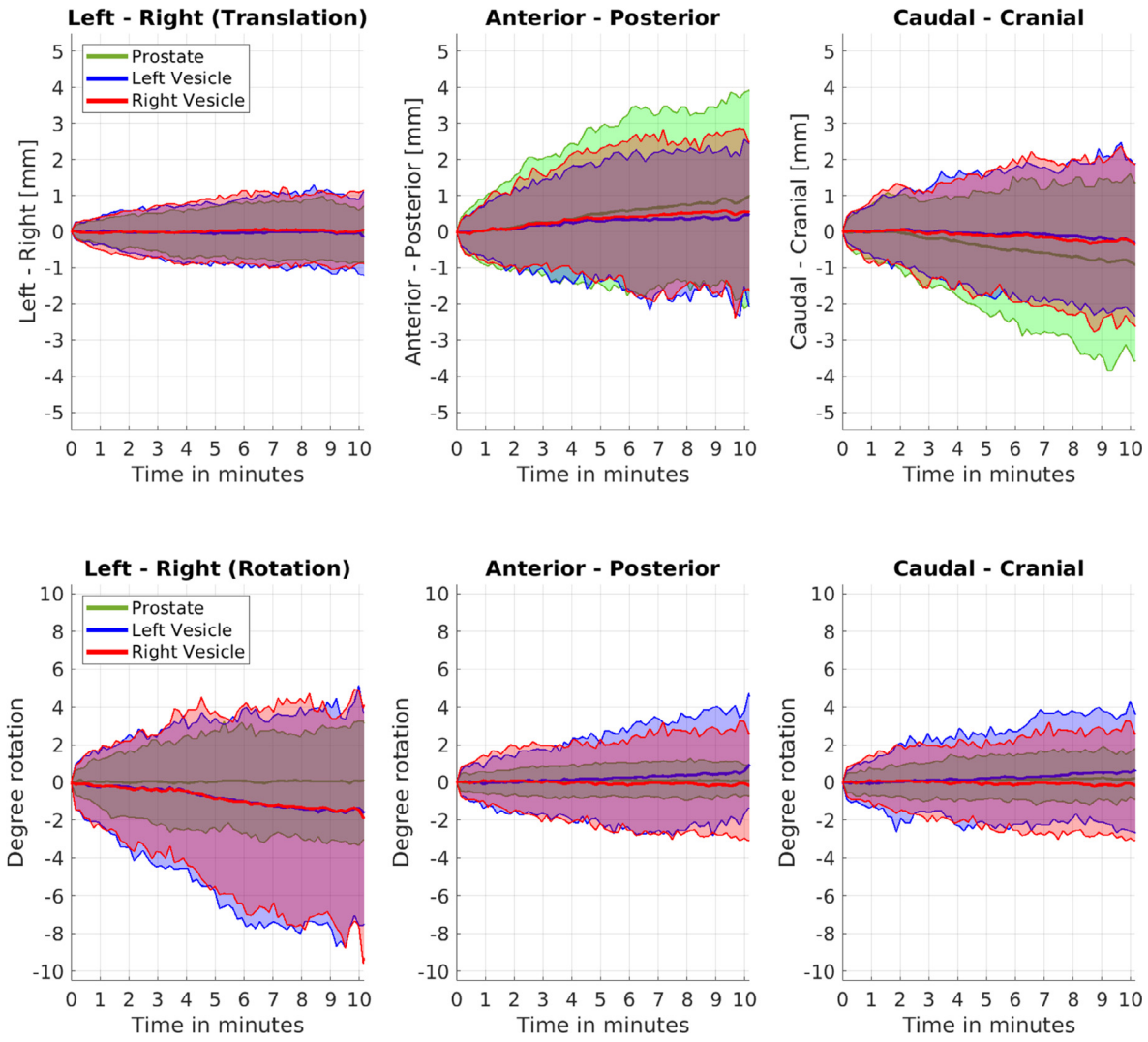

Fig. 2. Overview of the population translation and rotation results, with the intrafraction motion of the prostate (green), left seminal vesicle (blue) and right seminal vesicle (red). The area containing the 90 percentile intervals are shown as the clouds in the respective colors. The lines in the respective colors in the center of these areas describe the population mean. Results provided over 247 fractions and 50 patients and these results describe intrafraction motion during each fraction with respect to the first cine-MR dynamic acquired in that fraction.

Fig. 3. The case with the gas pocket as plotted in Fig. 3 is also provided as a movie as part of the supplementary material.

A visual example of the principle of the isometric volume expansion analysis is provided in Fig. 4. The prostate and vesicles can be seen reaching outside the 5 mm boundaries as an effect of intrafraction motion. Results from the corresponding coverage probability analysis show that 99% of the percentage of volume of the seminal vesicles can be covered at least 95% of the time when using 5 mm isometric volume expansion (Table 2).

Table 1
Classification of the types of major motion components seen for the intrafraction motion of the seminal vesicles.

Type of major motion component	Seen in fractions (%)	Seen in number of patients (%)
Gas pockets	18%	50%
Drift	30%	76%
Peristalsis	40%	84%
Stable	12%	32%

Discussion

When observing the intrafraction motion as provided in Fig. 2, it can be seen that seminal vesicle intrafraction motion in the left–right and anterior translation direction is similar to the prostate, while the prostate shows larger spread in the posterior and caudal direction. In addition, the seminal vesicles show slightly larger spread than the prostate in the cranial direction, but not in the caudal direction. Both the intrafraction motion of the seminal vesicles and prostate increases over time. Similar findings were reported by Gill et al. [11] using a 2D cine-MR based study. They reported that the seminal vesicles move significantly more than the prostate in the cranial-caudal direction but not in the anterior-posterior or left–right direction.

The spread in seminal vesicle movement in the cranial direction as observed from Fig. 2 might be a reflection of how seminal vesicles are affected by rectum filling variation or gas pockets. These effects tend to push the seminal vesicles in the anterior and cranial direction. Similar observations were reported by Sheng et al. [10]. Influences from gas pockets on the seminal vesicles were observed in 18% of the fractions (Table 1). This motion is often combined

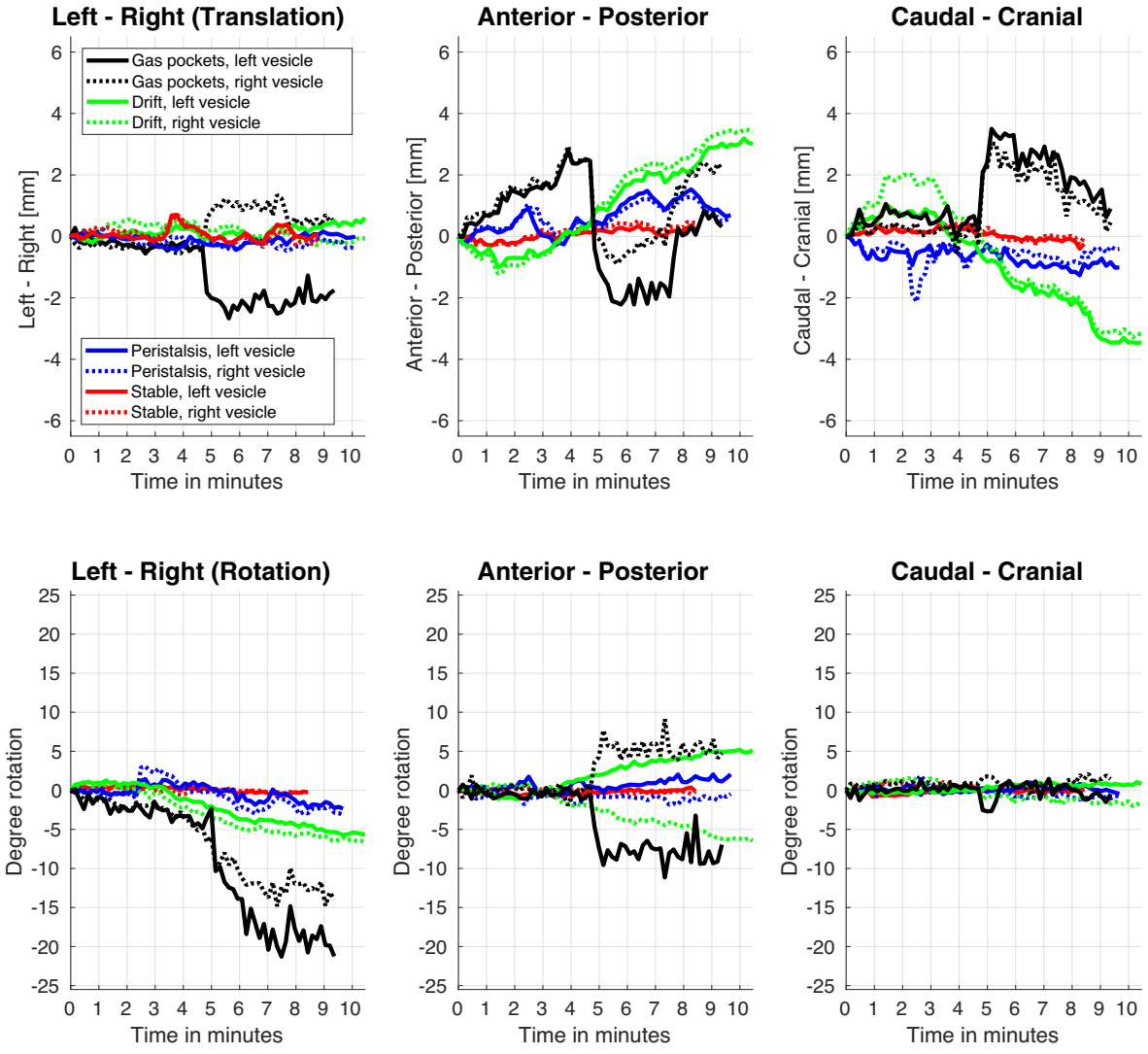

Fig. 3. Examples of different motions paths. An example for a patient with a gas pocket is shown in black, while an example with drift is shown in green, peristalsis in blue and stable in red. The motion paths for the left seminal vesicle are shown as continues lines, while motion paths for the right seminal vesicle are shown as the dashed lines.

with a rotation about the left–right axis, and this effect can be observed in the graph of Fig. 2. In this graph, the spread in seminal vesicle motion is significantly larger than observed for the prostate. The spread in intrafraction rotation for the seminal vesicles is also significantly larger than observed for the prostate about the anterior-posterior and caudal-cranial axis. The fact that the seminal vesicles are more easily influenced by changes in the rectum as they are anatomically positioned partly surrounding the rectum, can be recognized from the rotation graphs. Previous studies showed that the seminal vesicle position was primarily affected by rectal gas, while a correlation with bladder volume was not as strong [10,19]. However, Mak et al. [19] reported that a strong correlation of seminal vesicle anterior-posterior movement with the position of the most posterior point of the bladder was observed. Smitsmans et al. [20], quantified interfraction displacement of seminal vesicles using CBCT and reported a squared Pearson correlation coefficient (R^2) between the left and right seminal vesicle in the anterior-posterior direction of 0.62 (Pearson's r = 0.79). They reported that no correlation between the seminal vesicles for the left–right displacement was found, while caudal-cranial translations were not considered in the study. Liang et al. [21] found a R^2 value of 0.7 (Pearson's r = 0.84) between the anterior-posterior motion of the prostate and seminal vesicles. In addition, they reported that no correlation was found in the other directions. In our study we found Pearson correlation coefficients in the range of 0.72–0.76 for the left and right seminal vesicle with respect to the prostate in anterior-posterior and caudal-cranial translation direction (table S2). However, rotation correlation coefficients of the seminal vesicles with respect to the prostate were weak (table S2). Moreover, the Pearson's 95% confidence intervals indicate that the correlation differs per patient and that some patients have a very weak or none correlation. These confidence intervals indicate that it is useful to investigate seminal vesicle intrafraction motion for each individual patient specifically. The presented results show that the seminal vesicles move partly independently from the prostate, and our findings are consistent with previous studies [22,20,21,23–25,11].

An example of the intrafraction motion paths due to a gas pocket is visualized as the black traces in Fig. 3. In this figure, it can be observed that a gas pocket appears near the timepoint of 4-5 min leading to sudden translation displacements. The motion paths in the left–right translation graph show that both seminal vesicles were displaced laterally, in addition to displacement in the anterior and cranial translation direction. Significant rotation

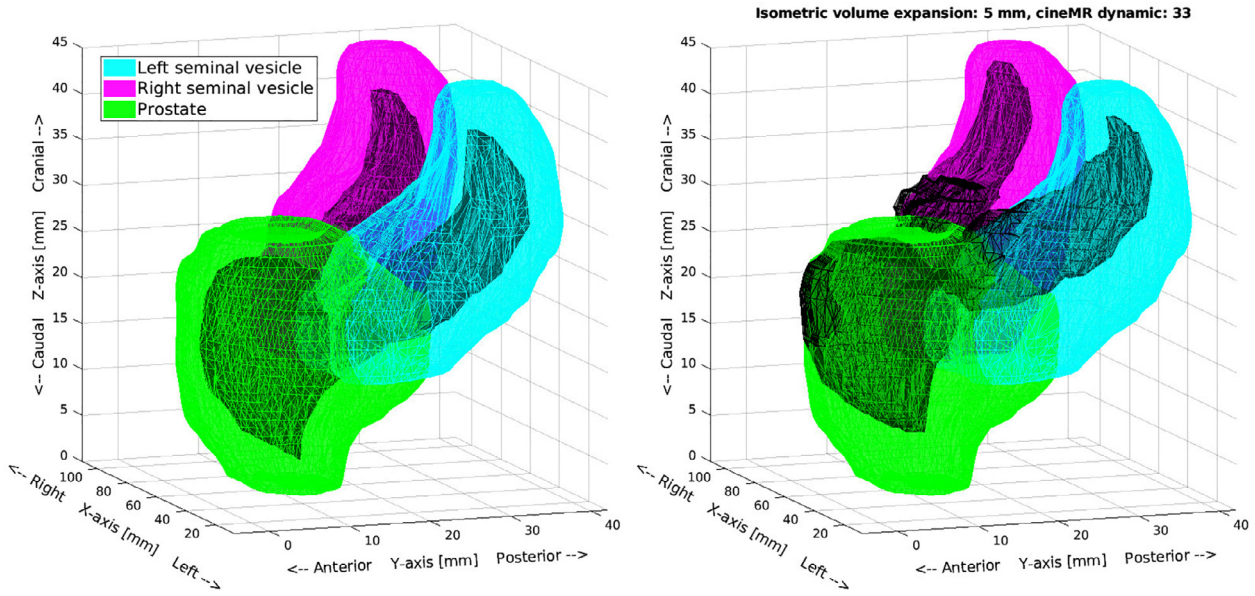

Fig. 4. Visualized example showing the volume expansion of 5 mm for the seminal vesicles (left seminal vesicle: cyan, right seminal vesicle: magenta) and prostate (green). The dark area in the graph on the left hand side visualizes the initial position of each target on the first cine-MR dynamic. The position of the targets due to intrafraction motion captured in a certain cine-MR frame is visualized as the dark areas in the graph on the right-hand side. In this graph can be observed that the targets reach outside the 5 mm boundaries used in this example.

about the left–right axis can be observed, combined with rotation about the anterior-posterior rotation axis due to rectal expansion.

A total of 16 cine-MR dynamics were removed due to misregistrations. All misregistrations occurred in cases where a large gas pocket was present. These gas pockets caused not only significant intrafraction motion of the seminal vesicles, but also led to local signal intensity artifacts which partly overlapped the seminal vesicles. This effect hindered the registration algorithm and led to inaccurate determination of the seminal vesicle location in these dynamics. However, in all cases the gas pocket passed after a few (range 1–5) dynamics (<1 min) after which the registration algorithm was able to continue registration. Banding artifacts may occur in bTFE sequences due to presence of rectal gas, however in this study we did not observe other significant influences of banding artifacts than the previously stated cases. Moreover, a bandwidth of 434 Hz/px (table S1) was used which was deemed sufficient to suppress the influence of any geometric distortions in the target area. Next, we did not observe significant influences of sudden motion on the acquired contrast or blurring/ghosting artifacts in the cine-MR dynamics. All reported misregistrations in this study were flagged by the adopted Kalman filter. We therefore propose that this filter could be used to identify sudden transitions that could lead to erroneous tracking results. In addition, the filter could also be used as a trigger for beam interruption.

Table 2
Results from the coverage probability analysis using isometric volume expansion, providing the percentage of volume which is covered at least 95 percent of the time. Isometric volume expansion with the listed values was applied to the original masks created by the clinician on the first cine-MR dynamic of every fraction.

Isometric volume expansion	Left Seminal Vesicle percentage of volume covered ⩾95% of time	Right Seminal Vesicle percentage of volume covered ⩾95% of time	Prostate percentage of volume covered ⩾95% of time
1 mm	89.0	87.7	97.4
2 mm	94.6	93.7	98.7
3 mm	97.5	96.8	99.3
4 mm	98.8	98.4	99.7
5 mm	99.4	99.1	99.9
6 mm	99.8	99.6	99.9
7 mm	99.9	99.8	100
8 mm	99.9	99.9	100
9 mm	100	100	100
10 mm	100	100	100

The presented results are based on rigid registration with seminal vesicle specific masks. While deformation of the seminal vesicles is seen, this deformation mainly occurs near the seminal vesicles tips, away from the prostate corpus. Most deformation was observed in the anterior-posterior and cranial-caudal direction due to variation of bladder and rectal filling, which is similar to a previous study on seminal vesicle deformations assessed on repeat computed tomography (CT) by van der Wielen et al. [23]. In their study, deformation of the prostate and seminal vesicles relative to intraprostatic fiducial markers was determined based on CT. They observed the largest seminal vesicle shape variations on the posterior side of the seminal vesicles, followed by shape variations of the seminal vesicle tips. Similar findings were noted by Stenmark et al. [25], who concluded that the seminal vesicles exhibit greater variation with increasing distance from the prostate. These conclusions coincide with our findings on seminal vesicle rotations. Due to the favct that the seminal vesicles are connected to the prostate, largest seminal vesicle displacements were found towards the seminal vesicle tips.

However, reduced accuracy in tracking seminal vesicle tips due to deformation would not necessarily pose a problem. Kestin et al. [9] performed a pathologic analysis to determine the length of tumor involvement in the seminal vesicles. They found a median length of seminal vesicle involvement of 1.0 cm, while in 90% of the positive cases this was limited to the proximal 2.0 cm. In addition, van der Burgt et al. [26] studied the impact of tumor invasion on seminal vesicle mobility. They reported that increasing tumor invasion in the seminal vesicles reduces their mobility relative to the prostate corpus. Moreover, van der Burgt et al. [26] suggested that the flexibility of the seminal vesicles becomes smaller with increasing tumor infiltration. Based on our results and observations over all 247 fractions and 50 patients, we assume that the rigid registration method is sufficient to quantify seminal vesicle intrafraction motion. Even if the outer tip of a seminal vesicle is not completely accurately tracked, the obtained intrafraction

motion may still be deemed as sufficient accurate as it is based on the main body of the seminal vesicle.

The performed coverage probability analysis was based on the observed motion during the beam-on period of 10 min. Motion which occurred during the preparation and (re) planning phase was not included in this analysis. This approach assumes that any intrafraction motion occurring between the daily pre-treatment scan and the beam-on period was negated. The results as presented in Table 2 show that 99% of the volume of both the left and right seminal can be covered at least 95% of the time when using 5 mm isometric volume expansion. In the case of the prostate, this threshold can be reached when using 3 mm isometric volume expansion. Especially the intrafraction rotation about the left–right axis has an effect on the coverage probability, as the rotation about this axis requires larger volumetric expansion to provide sufficient coverage.

The results indicate that the seminal vesicles do not move identically. This can be observed from Fig. 2, in which the right seminal vesicle has slightly larger spread in the posterior translation direction compared to the left seminal vesicle. The difference between the left and right seminal vesicle may be attributed to the asymmetrical shape and positioning of the rectum. Furthermore, it can be observed from the rotation graphs in Fig. 2 and 3 that the seminal vesicles are negatively correlated in the anterior-posterior and caudal-cranial rotation axis. This effect is most easily seen in Fig. 3, in the graph of rotation about the anterior-posterior axis. In this graph, the seminal vesicles seem to diverge, were for the (e.g.) drift case the left seminal vesicle shows positive rotation, while the right seminal vesicle shows negative rotation. This effect may also be seen in the population mean lines of Fig. 2, in the graphs of rotation about the anterior-posterior and caudal-cranial axis. In these graphs, the population mean lines of the seminal vesicles diverge over time. This is supported by the reported Pearson's correlation coefficients of −0.58 for the anterior-posterior and −0.47 for the caudal-cranial rotation. All these results indicate that the seminal vesicles rotate in opposite directions about the anterior-posterior and caudal-cranial axes when they are pushed by the rectum.

The here presented tracking method may be used as input for a fast replanning algorithm, which allows for intrafraction plan adaption. Examples of such replanning algorithms are described by Kontaxis et al. [27,28]. Application of such methods may provide opportunities to treat high-risk prostate cancer patients with ultra-hypofractionated radiotherapy (1–2 fractions).

To conclude, this is the first study to investigate six dimensions of freedom seminal vesicle intrafraction motion from 3D cine-MR imaging during actual treatments. We have shown that seminal vesicle intrafraction motion can be determined using a rigid registration method. Seminal vesicle intrafraction motion is larger than prostate intrafraction motion in the cranial direction, but not in the left–right and anterior-posterior direction. In addition, significant larger spread in rotations about the left–right, anterior-posterior and caudal-cranial axes was found for the seminal vesicles relative to the prostate. The results have shown that in the case of intrafraction motion correction for MR-guided radiotherapy not only translation, but especially seminal vesicle rotation should be corrected for when including seminal vesicles as target. With the gained insight on seminal vesicle intrafraction motion we will proceed towards MR-guided hypofractionated radiotherapy for intermediate and high-risk prostate cancer patients.

Declaration of Competing Interest

The authors declare that they have no known competing financial interests or personal relationships that could have appeared to influence the work reported in this paper.

Acknowledgments

The department of radiotherapy has a research agreement with Elekta. This research received no funding or financial compensation from Elekta. This work received financial support by ZonMw IMDI/LSH-TKI foundation projectnr. 104006004.

Appendix A. Supplementary data

Supplementary data associated with this article can be found, in the online version, at https://doi.org/10.1016/j.radonc.2021.07.014.

References

[1] Prostate Radiotherapy Integrated With Simultaneous MRI (The PRISM Study) (PRISM). https://clinicaltrials.gov/ct2/show/NCT03658525..
[2] Dunlop A, Mitchell A, Tree A, Barnes H, Bower L, Chick J, et al., Daily adaptive radiotherapy for patients with prostate cancer using a high field mr-linac: Initial clinical experiences and assessment of delivered doses compared to a c-arm linac, Clinical and Translational Radiation Oncology..
[3] Tetar SU, Bruynzeel AM, Lagerwaard FJ, Slotman BJ, Bohoudi O, Palacios MA. Clinical implementation of magnetic resonance imaging guided adaptive radiotherapy for localized prostate cancer. Phys Imaging Rad Oncol 2019;9:69–76.
[4] Alongi F, Rigo M, Figlia V, Cuccia F, Giaj-Levra N, Nicosia L, et al. 1.5 t mr-guided and daily adapted sbrt for prostate cancer: feasibility, preliminary clinical tolerability, quality of life and patient-reported outcomes during treatment. Rad Oncol 2020;15:1–9.
[5] de Muinck Keizer DM, Kerkmeijer LG, Willigenburg T, van Lier AL, den Hartogh MD, van Zyp JvdV, Prostate intrafraction motion during the preparation and delivery of MR-guided radiotherapy sessions on a 1.5T MR-Linac, Radiotherapy and Oncology 151 (2020) 88–94..
[6] Kontaxis C, de Muinck Keizer DM, Kerkmeijer LG, Willigenburg T, den Hartogh MD, de Groot-van Breugel EN, et al. Delivered dose quantification in prostate radiotherapy using online 3d cine imaging and treatment log files on a combined 1.5 t magnetic resonance imaging and linear accelerator system, Physics and Imaging. Rad Oncol 2020;15:23–9.
[7] Menten MJ, Mohajer JK, Nilawar R, Bertholet J, Dunlop A, Pathmanathan AU, et al. Automatic reconstruction of the delivered dose of the day using mr-linac treatment log files and online mr imaging. Radiother Oncol 2020;145:88–94.
[8] Ghilezan MJ, Jaffray DA, Siewerdsen JH, Van Herk M, Shetty A, Sharpe MB, et al. Prostate gland motion assessed with cine-magnetic resonance imaging (cine-mri). Int J Rad Oncol Biol Phys 2005;62:406–17.
[9] Kestin LL, Goldstein NS, Vicini FA, Yan D, Korman HJ, Martinez AA. Treatment of prostate cancer with radiotherapy: should the entire seminal vesicles be included in the clinical target volume? Int J Rad Oncol Biol Phys 2002;54:686–97.
[10] Sheng Y, Li T, Lee WR, Yin F-F, Wu QJ. Exploring the margin recipe for online adaptive radiation therapy for intermediate-risk prostate cancer: an intrafractional seminal vesicles motion analysis. Int J Rad Oncol Biol Phys 2017;98:473–80.
[11] Gill S, Dang K, Fox C, Bressel M, Kron T, Bergen N, et al. Seminal vesicle intrafraction motion analysed with cinematic magnetic resonance imaging. Rad Oncol 2014;9:174.
[12] Raaymakers B, Jürgenliemk-Schulz I, Bol G, Glitzner M, Kotte A, Van Asselen B, et al. First patients treated with a 1.5 t mri-linac: clinical proof of concept of a high-precision, high-field mri guided radiotherapy treatment. Physics Med Biol 2017;62:L41.
[13] de Muinck Keizer DM, Kerkmeijer LG, Maspero M, Andreychenko A, van Zyp JvdV, Van den Berg CA, et al., Soft-tissue prostate intrafraction motion tracking in 3d cine-mr for mr-guided radiotherapy, Physics in Medicine & Biology 64 (23) (2019) 235008..
[14] Stroom JC, de Boer HC, Huizenga H, Visser AG. Inclusion of geometrical uncertainties in radiotherapy treatment planning by means of coverage probability. Int J Rad Oncol Biol Phys 1999;43:905–19.
[15] Baum C, Alber M, Birkner M, Nüsslin F. Robust treatment planning for intensity modulated radiotherapy of prostate cancer based on coverage probabilities. Radiotherapy Oncol 2006;78:27–35.
[16] de Muinck Keizer D, Pathmanathan A, Andreychenko A, Kerkmeijer L, van Zyp JvdV, Tree A, et al., Fiducial marker based intra-fraction motion assessment on cine-MR for MR-linac treatment of prostate cancer, Physics in Medicine & Biology 64 (7) (2019) 07NT02, doi: 10.1088/1361-6560/ab09a6..
[17] de Boer HC, Heijmen BJ, eNAL: an extension of the NAL setup correction protocol for effective use of weekly follow-up measurements, International Journal of Radiation Oncology* Biology* Physics 67 (5) (2007) 1586–1595, doi: 10.1016/j.ijrobp.2006.11.050..
[18] Van Herk M, Errors and margins in radiotherapy, in: Seminars in radiation oncology, Vol. 14, Elsevier, 2004, pp. 52–64..

[19] Mak D, Gill S, Paul R, Stillie A, Haworth A, Kron T, et al. Seminal vesicle interfraction displacement and margins in image guided radiotherapy for prostate cancer. Rad Oncol 2012;7:139.
[20] Smitsmans MH, De Bois J, Sonke J-J, Catton CN, Jaffray DA, Lebesque JV, Van Herk M. Residual seminal vesicle displacement in marker-based image-guided radiotherapy for prostate cancer and the impact on margin design. Int J Rad Oncol Biol Phys 2011;80:590–6.
[21] Liang J, Wu Q, Yan D. The role of seminal vesicle motion in target margin assessment for online image-guided radiotherapy for prostate cancer. Int J Rad Oncol Biol Phys 2009;73:935–43.
[22] Deurloo KE, Steenbakkers RJ, Zijp LJ, de Bois JA, Nowak PJ, Rasch CR. M. van Herk, Quantification of shape variation of prostate and seminal vesicles during external beam radiotherapy. Int J Rad Oncol Biol Phys 2005;61:228–38.
[23] van der Wielen GJ, Mutanga TF, Incrocci L, Kirkels WJ, Osorio EMV, Hoogeman MS, et al. Deformation of prostate and seminal vesicles relative to intraprostatic fiducial markers. Int J Rad Oncol Biol Phys 2008;72:1604–11.
[24] Mutanga TF, de Boer HC, van der Wielen GJ, Hoogeman MS, Incrocci L, Heijmen BJ. Margin evaluation in the presence of deformation, rotation, and translation in prostate and entire seminal vesicle irradiation with daily marker-based setup corrections. Int J Rad Oncol Biol Phys 2011;81:1160–7.
[25] Stenmark MH, Vineberg K, Ten Haken RK, Hamstra DA, Feng M. Dosimetric implications of residual seminal vesicle motion in fiducial-guided intensity-modulated radiotherapy for prostate cancer. Med Dosim 2012;37:240–4.
[26] van der Burgt M, Bergsma L, de Vries J, Pos FJ, Kalisvaart R, Heemsbergen W, Remeijer P, van der Heide UA. Impact of tumour invasion on seminal vesicles mobility in radiotherapy of prostate cancer. Radiother Oncol 2015;117:283–7.
[27] Kontaxis C, Bol G, Lagendijk J, Raaymakers B. A new methodology for inter-and intrafraction plan adaptation for the mr-linac. Phys Med Biol 2015;60:7485.
[28] Kontaxis C, Bol G, Stemkens B, Glitzner M, Prins F, Kerkmeijer L, Lagendijk J, Raaymakers B. Towards fast online intrafraction replanning for free-breathing stereotactic body radiation therapy with the mr-linac. Phys Med Biol 2017;62:7233.